

Bilayer Molecular Metals Based on Dissymmetrical Electron Donors

Sandrina Oliveira,[†] José Ministro,[†] Isabel C. Santos,[†] Dulce Belo,[†] Elsa B. Lopes,[†] Sandra Rabaça,^{*,†} Enric Canadell,[‡] and Manuel Almeida^{*,†}[†]C²TN, Instituto Superior Técnico, Universidade de Lisboa, Estrada Nacional 10, P-2695-066 Bobadela LRS, Portugal[‡]Institut de Ciència de Materials de Barcelona (ICMAB-CSIC), Campus UAB, E-08193 Bellaterra, Spain

Supporting Information

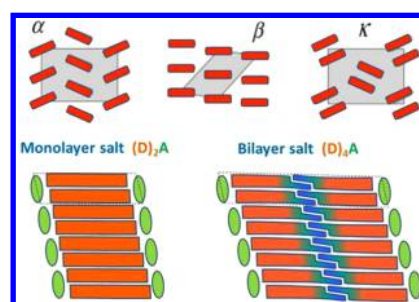
ABSTRACT: The electrocrystallization from solutions of cyanobenzene-ethylenedithio-tetrathiafulvalene (CNB-EDT-TTF) in the presence of different anions X = ClO₄⁻, PF₆⁻, and I₃⁻, affords a new type of 2D molecular metals with composition (CNB-EDT-TTF)₄X based on an unprecedented bilayer structure of the donors induced by effective head to head interdonor interactions through the nitrile groups, which is responsible for 2D metallic systems with unusual properties such as the higher band filling, larger effective mass of carriers, and almost degenerated double Fermi surfaces.

TTF derivatives have been at the basis of the majority of the organic conductors, reported in the last decades.¹ An early trend soon established after the discovery of first organic metals and superconductors in the development of new electronic materials of this type was the preparation of electroactive molecules based on sulfur rich and extended π -systems capable to establish in the solid state interactions in more than one direction. The most successful molecular building blocks for this type of electronic materials have been sulfur and other chalcogen rich derivatives of TTF such as bis-ethylenedithio tetrathiafulvalene (ET) in salts with composition (ET)₂X where X can be a diversity of monoanions.² Indeed this type of molecules has provided not only the large majority of organic metals and superconductors presently known but also many two-dimensional solids with a very rich diversity of electronic ground states, from superconducting, to insulating, antiferromagnetic, etc.^{2,3}

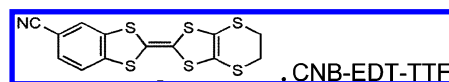
The crystal structures of these salts have a strong 2D character with donor molecules packed with their long axis parallel to each other in layers that alternate with anionic layers. The way the molecules are packed in a layer can be quite diverse,⁴ leading to a very rich variety of electronic properties. The most common structures associated with metallic and superconducting properties are the α -, β -, and κ -phases depicted in Scheme 2. During the past few years some salts of this type of donors were found to present more complex structures where two different donor layers may alternate in the solid,⁵ but in all cases the layers have a thickness corresponding to the length of one donor molecule (monolayers).

We recently developed the dissymmetrical ET derivative cyanobenzene-ethylenedithio-tetrathiafulvalene (CNB-EDT-TTF)⁶ (Scheme 1), which through a weak hydrogen bond assisted interaction is capable to form effective dimeric interactions promoting the crystallization of its charge transfer

Scheme 2. 2D Packing Patterns of Donor Molecules (Top); Monolayer and Bilayer Structure of Charge Transfer Salts (Bottom)



Scheme 1. CNB-EDT-TTF Molecular Structure



salts with several small anions X into a new type of bilayer structures (Scheme 2) with metallic properties and composition (CNB-EDT-TTF)₄X.

Electrocrystallization of CNB-EDT-TTF from dichloromethane in the presence of salts of perchlorate, hexafluorophosphate, and triiodide leads to dark brown platelet crystals with metallic shine. Well-formed crystals are only obtained using moderate current densities ($\sim 1 \mu\text{A}/\text{cm}^2$). Larger currents lead to a dark powder material with ill-defined composition, suggesting that after the oxidation of a donor molecule at the electrode the growth of salts with 4:1 donor to acceptor stoichiometry requires the association with neutral molecules in solution to allow the formation of partially oxidized tetrameric units (CNB-EDT-TTF)₄⁺. Larger current probably does not allow the relatively slow, diffusion controlled, higher association process (Scheme S1).

Two distinct structural bilayer types have been observed in (CNB-EDT-TTF)₄X salts. For X = PF₆⁻ (1) and ClO₄⁻ (2), the crystal structure is triclinic $P\bar{1}$ with one independent donor molecule per asymmetric unit.⁷ The donor molecules present in each layer an arrangement of β' -type as observed in many ET salts with all molecules with the same orientation and conformation disorder in the dithiine ring in 1 (Figure S1a). The layers are however coupled in bilayers through the nitrile groups all pointing to the same side of the layers. The nitrile

Received: June 1, 2015

Published: June 30, 2015

groups through dipolar and bifurcated C–N⋯H interactions provide a very effective way of pair association of the molecules between adjacent layers (Figures 1 and S2–S8). The head to

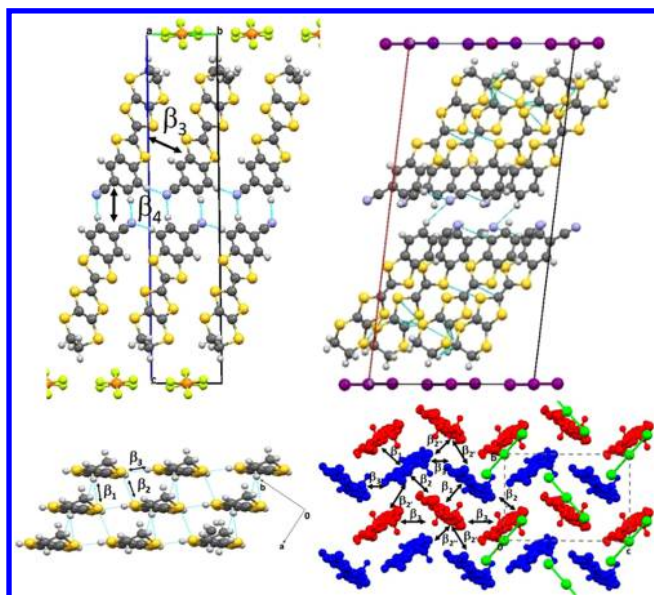


Figure 1. Crystal structure of **1** (left) and **3** (right); viewed along the *a* and *b* axis, respectively (top), and partial view of one donor layer along the long axis of molecules (bottom). The arrows denote the different intermolecular interactions.

head coupling of two almost coplanar molecules in different layers can be described as a dimeric $R^2_2(10)$ homosynthon. In addition, through the bifurcated C–N⋯H interaction, there is a side coupling between two molecules in each layer, which can be described as a $R^2_4(10)$ synthon (Figure S8). Although the C–N⋯H interactions are relatively weak it is worth referring that they are rather common among molecules with nitrile moieties.

The octahedral PF_6 anions present anomalous large displacement parameters with ill-defined positions (Figure S1) and low occupation factors corresponding to 0.5 atoms. The tetrahedral ClO_4 anions appear disordered over two almost equally populated positions slightly displaced along the *a*-axis, denoting both position disorder of the Cl atom and orientation disorder of the oxygen atoms in the interlayer cavities (Figure S3). This disorder is not so common in ET monolayer salts and may result from a weak correlation between the anion in different layers.

For $X = I_3^-$ (**3**), the crystal is monoclinic $P2_1/c$ with two independent donor molecules per asymmetric unit.⁸ The donor molecules are arranged head to head in layers with a *k*-type arrangement, and again the layers are coupled in bilayers by identical C–N⋯H interactions with $R^2_2(10)$ and $R^2_4(10)$ synthons, which now involve nonequivalent molecules (Figures S6 and S8). In this compound as a consequence of the κ -type packing the $R^2_4(10)$ synthon involves molecules with a significant tilting angle at variance with the compounds **1** and **2** where the molecules were essentially coplanar. The two donor units within experimental uncertainty have identical molecular parameters, although one of them is closer to the anion positions than the other. The anions appear also as disordered among two possible orientations. Iodine atom I3 and I1 lie at the inversion center with occupation factors of 0.467 and 0.033. These two positions correspond to two different orientations of triiodide anions (Figure S5). In Figure 1 (bottom right) only the major

orientation is represented. Again this disorder may also denote a weak correlation between the anion positions in different layers.

Both the structural refinement, in spite of the anion disorder, and the results of microprobe EDS analysis are consistent with a 4:1 stoichiometry. This unusual donor/anion 4:1 stoichiometry instead of the standard 2:1 observed in analogous single layered salts is easy to understand as a direct consequence of the bilayer structure with anionic layers identical to the single layer structures (see Scheme 2).

The electronic properties of these bilayer salts can be understood in terms of the electronic band structure, which can be easily estimated from the crystal structure using the extended Hückel approach,⁹ which, in spite of its simplicity, has been quite successful in describing the properties of molecular conductors (Figure 2).¹⁰ The relevant $\beta_{\text{HOMO-HOMO}}$ intermo-

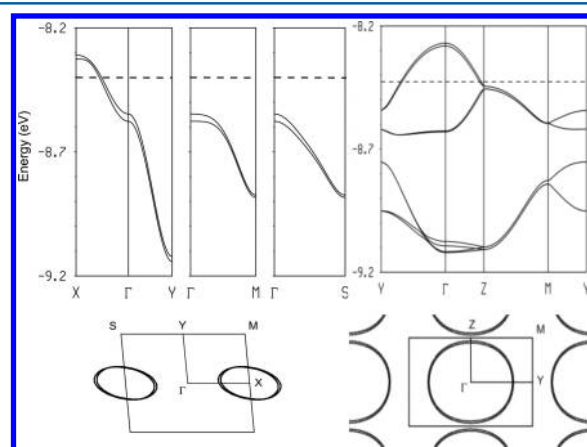


Figure 2. Calculated electronic band structure (top) and Fermi surface (bottom) of **1** (left) and **2** (right).

lecular interaction energies,¹¹ which are a measure of the strength of the interaction between the HOMO of the different donor molecules in the crystal structure, have been calculated using a double- ζ basis set¹² and are reported in Table 1.

Table 1. Absolute Values of $\beta_{\text{HOMO-HOMO}}$ Intermolecular Interaction Energies (meV) in $(\text{CNB-EDT-TTF})_4X$ Crystals

X	PF_6	ClO_4	I_3		
			β	β'	β''
β_1	116.5	112.7	301.5		
β_2	219.1	233.7	139.2	167.6	128.7
β_3	52.7	50.7	79.2	40.6	
β_4	3.1	2.7	1.8		

In the ClO_4^- and PF_6^- salts with only one independent donor molecule and a β -type packing, besides the intermolecular interactions between molecules in the same layer, β_1 , β_2 , β_3 , characteristic of the β'' -type packing, there is a smaller interaction β_4 between almost coplanar molecules in nearby layers connected through the C–N⋯H interactions. As a consequence of this interlayer interaction β_4 the usual 2D dispersive band is split into two closely spaced bands filled up to approximately 7/8, and the Fermi surface is two closely spaced cylinders with an area corresponding to almost 1/8 of the first Brillouin zone as shown in Figure 2.

In the I_3^- salt there are four donor units in the unit cell of each layer (two inequivalent, depicted in red and blue in Figure 1)

with a κ -type donor packing. The relevant distinct intermolecular interactions between molecules in the same layer now six ($\beta_1, \beta_2, \beta_2', \beta_3, \beta_3'$), identified in Figure 1 (bottom right). There is also a weaker interaction (β_4) between two inequivalent molecules in different layers, connected by the C–N...H interactions (Figure S6). The four donors per unit cell in each layer lead to four HOMO bands, which due to the weaker interlayer interaction t_4 are split each in two almost degenerated ones. The upper pair of bands are close to half filled. The corresponding Fermi surfaces are two closely spaced cylinders with an area corresponding to almost 1/2 of the first Brillouin zone.

The calculated electronic band structure of these compounds is confirmed by their electrical transport properties. The electrical conductivity measured in single crystals along their long axis b is of the order of 18, 22, and 28 S/cm for the ClO_4 , PF_6 , and I_3 salts, respectively. In spite of the modest room temperature values, the conductivity presents in all cases a metallic behavior with a smooth decrease upon cooling (Figure 3). This decrease is almost proportional to temperature with the

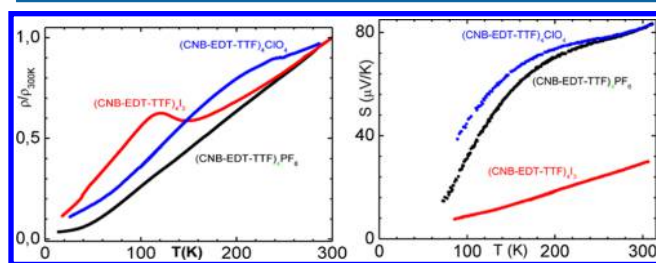


Figure 3. Electrical resistivity ρ (left) and absolute thermopower S (right) of 1, 2, and 3 single crystals as a function of temperature T .

exception of a smooth anomaly between 110 and 140 K in 3 and an anomaly near 250 K for 2, possibly associated with donor charge and anion ordering, respectively. Thermoelectric power measurements decreasing toward zero upon cooling confirm the metallic behavior of these compounds (Figure 3). The large values of the ClO_4 and PF_6 salts, $\sim 82 \mu\text{V/K}$ at 300 K, very large for a metallic system, are the result of a highly filled (7/8) band, while the smaller values of the iodine salt, $\sim 28 \mu\text{V/K}$ at 300 K, are consistent with a system close to half filled, as predicted by the band calculations. Further studies at lower temperatures and under magnetic field are expected to confirm the above details of the band structure.

In conclusion we have shown how the nonsymmetrically cyano-substituted TTF derivative CNB-EDT-TTF can originate a new type of 2D metallic charge transfer salts with compositions $(\text{CNB-EDT-TTF})_4\text{X}$ ($\text{X} = \text{ClO}_4^-, \text{PF}_6^-, \text{and } \text{I}_3^-$), based on a novel bilayer structure of the donors. The bilayer structure is induced by effective head to head interactions through the nitrile groups. These salts are certainly just the first examples of a new generation of molecular conductors expected to be obtained in the future with other anions, where interesting effects resulting from the higher band filling are expected to occur.

■ ASSOCIATED CONTENT

Supporting Information

Experimental and crystallography details, band structure calculations for 2, and CIF files for 1, 2, and 3. The Supporting Information is available free of charge on the ACS Publications website at DOI: 10.1021/acs.inorgchem.5b01240.

■ AUTHOR INFORMATION

Corresponding Authors

*E-mail: sandrar@ctn.ist.utl.pt.

*E-mail: malmeida@ctn.ist.utl.pt.

Notes

The authors declare no competing financial interest.

■ ACKNOWLEDGMENTS

This work was partially supported by FCT (Portugal) under contracts PTDC/QEQ-SUP/1413/2012, UID/Multi/04349/2013, and RECI/QEQ-QIN/0189/2012 and Ph.D. grant to S.O. (SFRH/BD/72722/2010). Work in Bellaterra was supported by MINECO-Spain (Grant FIS2012-37549-C05-05) and Generalitat de Catalunya (2014SGR301).

■ REFERENCES

- (a) Bendikov, M.; Wudl, F.; Perepichka, D. F. *Chem. Rev.* **2004**, *104*, 4891–4946. (b) Yamada, J. In *TTF Chemistry Fundamentals and Applications of Tetrathiafulvalene*; Sugimoto, T., Ed.; Kodansha and Springer: Tokyo, 2004.
- (a) Bernier, P.; Lefrant, S.; Bidan, G., Eds. *Advances in Synthetic Metals, Twenty Years of Progress in Science and Technology*; Elsevier: Amsterdam, 1999. (b) Ishiguro, T.; Yamaji, K.; Saito, G. *Organic Superconductors*, 2nd ed.; Springer-Verlag: Berlin, 1998.
- (a) Seo, H.; Hotta, C.; Fukuyama, H. *Chem. Rev.* **2004**, *104*, 5005–5036. (b) Jerome, D. *Chem. Rev.* **2004**, *104*, 5565–5591.
- (a) Mori, T. *Bull. Chem. Soc. Jpn.* **1998**, *71*, 2509–2526. (b) Mori, T.; Mori, H.; Tanaka, S. *Bull. Chem. Soc. Jpn.* **1999**, *72*, 179–197. (c) Mori, T. *Bull. Chem. Soc. Jpn.* **1999**, *72*, 2011–2027.
- (a) Schlueter, J. A.; Wiehl, L.; Park, H.; de Souza, M.; Lang, M.; Koo, H.; Whangbo, M. J. *Am. Chem. Soc.* **2010**, *132*, 16308–16310. (b) Lyubovskaya, R.; Zhilyaeva, E.; Shilov, G.; Audouard, A.; Vignolles, D.; Canadell, E.; Pesotskii, S.; Lyubovskii, R. *Eur. J. Inorg. Chem.* **2014**, 3820–3836. (c) Shin, K.-S.; Jeannin, O.; Brezgunova, M.; Dahaoui, S.; Aubert, E.; Espinosa, E.; Auban-Senzier, P.; Świetlik, R.; Frąckowiak, A.; Fourmigué, M. *Dalton Trans.* **2014**, 43, S280–S291. (d) Prokhorova, T. G.; Buravov, L. I.; Yagubskii, E. B.; Zorina, L. V.; Simonov, S. V.; Shibaeva, R. P.; Zverev, V. N. *Eur. J. Inorg. Chem.* **2014**, 2014, 3933–3940.
- Oliveira, S.; Belo, D.; Santos, I. C.; Rabaça, S.; Rabaça, S.; Almeida, M. *Beilstein J. Org. Chem.* **2015**, *11*, 951–956.
- See Table S1 for detailed Crystallographic data for compounds 1 and 2. Additional selected bond lengths and selected short contacts can be found in Tables S2–S3 and Tables S4–S5 for compounds 1 and 2, respectively.
- See Table S1 for detailed crystallographic data of 3. Additional selected bond lengths, angles, and selected short contacts can be found in Tables S6–S7. Crystallographic details and a more detailed discussion are given in the Supporting Information.
- (a) Whangbo, M.-H.; Hoffmann, R. *J. Am. Chem. Soc.* **1978**, *100*, 6093–6098. (b) Ammeter, J. H.; Bürgi, H.-B.; Thibeault, J.; Hoffmann, R. *J. Am. Chem. Soc.* **1978**, *100*, 3686–3692. (c) Ren, J.; Liang, W.; Whangbo, M.-H. *Crystal and Electronic Structure Analysis Using CAESAR*; PrimeColor Software, Inc.: Cary, NC, 1998.
- Wosnitza, J. *Fermi Surfaces of Low-Dimensional Organic Metals and Superconductors*; Springer-Verlag: Berlin, 1996.
- Whangbo, M.-H.; Williams, J. M.; Leung, P. C. W.; Beno, M. A.; Emge, T. J.; Wang, H. H. *Inorg. Chem.* **1985**, *24*, 3500–3502.
- (a) Canadell, E.; Rachidi, I.E.-I.; Ravy, S.; Pouget, J. P.; Brossard, L.; Legros, J. P. *J. Phys. (Paris)* **1989**, *50*, 2967. (b) Baudron, S.; Avarvari, N.; Canadell, E.; Auban-Senzier, P.; Batail, P. *Chem. - Eur. J.* **2004**, *10*, 4498–4511.